

# Resonance wave functions located at the Stark saddle point

Holger Cartarius,\* Jörg Main, Thorsten Losch, and Günter Wunner  
*Institut für Theoretische Physik 1, Universität Stuttgart, 70550 Stuttgart, Germany*  
(Dated: November 1, 2018)

We calculate quantum mechanically exact wave functions of resonances in spectra of the hydrogen atom in crossed external fields and prove the existence of long-lived decaying quantum states localized at the Stark saddle point. A spectrum of ground and excited states reproducing the nodal patterns expected from simple quadratic and cubic expansions of the potential in the vicinity of the saddle point can be identified. The results demonstrate the presence of resonances in the vicinity of the saddle predicted by simple approximations.

PACS numbers: 32.60.+i, 32.80.Fb, 82.20.Db

## I. INTRODUCTION

The hydrogen atom in crossed static electric and magnetic fields is an important example for a quantum system accessible both in experiments and numerical calculations. Adding external fields to the Coulomb potential of the hydrogen atom opens the possibility for wave functions to be localized far away from the nucleus. The existence of such localized states in quantum systems has attracted the attention of both theoretical [1–4] and experimental [5, 6] investigations over a long period of time. First investigations considered a gauge dependent variant of the system, in which the paramagnetic term was omitted [1, 2, 5] due to its smallness as compared with the diamagnetic term at large field strengths. The resulting sum potential possesses a minimum away from the nucleus in which localized states can exist. However, if one takes into account all terms of the magnetic field, one can immediately see that the outer potential minimum does not exist in the real physical system, rather, one finds classical electron motion close to the Stark saddle point which is bound in two directions and unbound in the third direction. In fact, localized resonance quantum states in the vicinity of the saddle point have been predicted by Clark et al. [4] as quantized version of this quasi-bound motion.

The question whether or not resonances located at the Stark saddle point do exist has also a crucial meaning for the ionization mechanism. Classical electron paths describing an ionization must pass the vicinity of the Stark saddle. This process was investigated, e.g., using the transition state theory [7–11]. The transition state theory is applicable to many dynamical systems which evolve from an initial to a final state and has its origin in the calculation of chemical reaction rates. The concept is based on classical trajectories which describe a reaction by passing a boundary in phase space, viz. the transition state, which must be crossed by all trajectories connecting the initial (“reactants”) and final (“products”) side. For the hydrogen atom in crossed fields the theory postu-

lates classical orbits confined in the vicinity of the Stark saddle point [7].

The work by Clark et al. [4] can be regarded as a first step in discussing the ionization mechanism of the hydrogen atom in crossed electric and magnetic fields in this context. The quasi-bound states confined to the vicinity of the saddle found by Clark et al. coincide with an approximation to the Hamiltonian in the framework of the transition state theory, however, only an algorithmic procedure based on a normal-form representation of a power-series expansion of the Hamiltonian allowed for identifying the transition state [7, 10, 11]. Even though the transition state for the hydrogen atom in crossed fields has been found, the question of whether or not the classical trajectories in its vicinity leave a signature in the exact quantum spectrum remained unanswered for a long time. Finally, clear evidence for signatures in the energies, i.e., the eigenvalues of the quantum resonances, was found [12].

It is the purpose of this paper to demonstrate that there is, indeed, a relationship between the exact quantum resonances and the quantized energy levels of the electron motion near the transition state due to a definite spatial restriction of the resonances’ probability density to a small region around the saddle. We calculate the position space representation of the corresponding wave functions and are able to show that they are clearly located in a vicinity of the Stark saddle point. From a quadratic approximation of the potential around the saddle point one expects a harmonic oscillator spectrum of energy levels and wave functions. We even find nodal patterns in the exact quantum states which correspond to “excited” states of the quadratic approximation, and thus demonstrate the usefulness of the simple approximation and the existence of the resonances predicted by a classical treatment of the system [4, 7].

In Sec. II we introduce the system as well as the second- and third-order power-series expansions of the potential in the vicinity of the Stark saddle point. Position space representations of exact quantum wave functions which prove the existence of resonances located closely at the position of the saddle are presented in Sec. III. Conclusions are drawn in Sec. IV.

\*Electronic address: Holger.Cartarius@itp1.uni-stuttgart.de

## II. HAMILTONIAN AND APPROXIMATIONS IN THE VICINITY OF THE STARK SADDLE POINT

### A. Hamiltonian and exact quantum calculations

In Hartree units the Hamiltonian of a hydrogen atom in crossed external fields with an electric field  $f$  orientated along the  $x$ -axis and a magnetic field along the  $z$ -axis represented by the vector potential  $\mathbf{A}$  has the form

$$H = \frac{1}{2}(\mathbf{p} + \mathbf{A})^2 - \frac{1}{r} + fx. \quad (1)$$

The parity with respect to reflections at the ( $z = 0$ )-plane is a good quantum number and allows considering states with even and odd  $z$ -parity separately.

It is a common and efficient method to rewrite the Schrödinger equation for numerical calculations in dilated semiparabolic coordinates [12, 13],

$$\mu = \frac{1}{b}\sqrt{r+z}, \quad \nu = \frac{1}{b}\sqrt{r-z}, \quad \varphi = \arctan \frac{y}{x}, \quad (2)$$

which yields

$$\begin{aligned} & \left\{ \Delta_\mu + \Delta_\nu - (\mu^2 + \nu^2) + b^4 \gamma (\mu^2 + \nu^2) i \frac{\partial}{\partial \varphi} \right. \\ & - \frac{1}{4} b^8 \gamma^2 \mu^2 \nu^2 (\mu^2 + \nu^2) - 2b^6 f \mu \nu (\mu^2 + \nu^2) \cos \varphi \left. \right\} \psi \\ & = \{-4b^2 + \lambda (\mu^2 + \nu^2)\} \psi \quad (3) \end{aligned}$$

with

$$\Delta_\varphi = \frac{1}{\varphi} \frac{\partial}{\partial \varphi} \varphi \frac{\partial}{\partial \varphi} + \frac{1}{\varphi^2} \frac{\partial^2}{\partial \varphi^2}, \quad \varphi \in \{\mu, \nu\}, \quad (4)$$

and the generalized eigenvalues  $\lambda = -(1 + 2b^4 E)$ , which are related to the energies  $E$  of the quantum states. The calculation of the resonances is done with a diagonalization of a matrix representation of the Schrödinger equation (3) and the complex rotation method [14–16]. The necessary complex scaling of the coordinates  $\mathbf{r}$  is introduced via the complex convergence parameter

$$b = |b| e^{i\vartheta/2}. \quad (5)$$

Resonances appear as complex eigenvalues  $E$ , where the real part of  $E$  represents the energy and the imaginary part is related to the width  $\Gamma = -2\text{Im}(E)$ .

An adequate complete basis for the matrix representation of the Schrödinger equation (3) is given by

$$|n_\mu, n_\nu, m\rangle = |n_\mu, m\rangle \otimes |n_\nu, m\rangle, \quad (6)$$

where  $|n_\varphi m\rangle$  are the eigenstates of the two-dimensional harmonic oscillator. The position space representation in dilated semiparabolic coordinates has the form

$$\begin{aligned} \psi_{n_\mu n_\nu m}(\mu, \nu, \varphi) &= \sqrt{\frac{[(n_\mu - |m|)/2]! [(n_\nu - |m|)/2]!}{[(n_\mu + |m|)/2]! [(n_\nu + |m|)/2]!}} \\ &\times \sqrt{\frac{2}{\pi}} f_{n_\mu m}(\mu) f_{n_\nu m}(\nu) e^{im\varphi} \quad (7a) \end{aligned}$$

with the “radial” wave functions

$$f_{nm}(\varrho) = e^{-\varrho^2/2} \varrho^{|m|} L_{(n-|m|)/2}^{|m|}(\varrho^2) \quad (7b)$$

expressed in terms of Laguerre polynomials  $L_n^\alpha(x)$ . Due to the complex scaling  $\mu$  and  $\nu$  become complex coordinates. In properly complex conjugated wave functions obtained with the complex rotation method one has to bear in mind that only the intrinsically complex parts have to be conjugated [16, 17], i.e., in the complex conjugated version  $\psi_{n_\mu n_\nu m}^*$  of the wave function (7a)  $e^{im\varphi}$  is replaced with  $e^{-im\varphi}$  and the “radial” parts  $f_{n_\mu m}(\mu)$ ,  $f_{n_\nu m}(\nu)$ , which become complex *only* by the complex scaling, are *not* conjugated.

It is very effective to perform the matrix setup of the Schrödinger equation (3) completely algebraically by expressing Eq. (3) in terms of harmonic oscillator creation and annihilation operators. Consequently, the expansion coefficients  $c_{in_\mu n_\nu m}$  of the eigenstates obtained in a matrix diagonalization

$$\Psi_i(\mu, \nu, \varphi) = \sum_{n_\mu, n_\nu, m} c_{in_\mu n_\nu m} \psi_{n_\mu n_\nu m}(\mu, \nu, \varphi), \quad (8a)$$

$$\Psi_i^*(\mu, \nu, \varphi) = \sum_{n_\mu, n_\nu, m} c_{in_\mu n_\nu m} \psi_{n_\mu n_\nu m}^*(\mu, \nu, \varphi) \quad (8b)$$

belong to position space wave functions (7a), which are normalized eigenstates of two coupled two-dimensional harmonic oscillators,

$$\begin{aligned} & \int_0^\infty d\mu \int_0^\infty d\nu \int_0^{2\pi} d\varphi \mu \nu \psi_{n_\mu n_\nu m}^*(\mu, \nu, \varphi) \psi_{n'_\mu n'_\nu m'}(\mu, \nu, \varphi) \\ & = \delta_{n_\mu n'_\mu} \delta_{n_\nu n'_\nu} \delta_{mm'}, \quad (9) \end{aligned}$$

but are not orthogonal and not normalized in the physical position space  $\mathbf{r} = (x, y, z)^\text{T}$ . The eigenstates (8a) and (8b) of the Schrödinger equation (3), however, can be normalized in such a way that

$$\begin{aligned} & \int d^3 \mathbf{r} \Psi_i^*(\mu, \nu, \varphi) \Psi_j(\mu, \nu, \varphi) \\ & = b^6 \int_0^\infty d\mu \int_0^\infty d\nu \int_0^{2\pi} d\varphi \mu \nu (\mu^2 + \nu^2) \Psi_i^* \Psi_j = \delta_{ij}. \quad (10) \end{aligned}$$

Since the proper complex conjugation of the wave functions effects only intrinsically complex parts, their square moduli must be replaced with  $\Psi_j^* \Psi_j$  as introduced in Eqs. (8a) and (8b) to obtain a measure for the probability density. For wave functions of decaying states this product will be complex, and we will visualize the modulus  $|\psi_{n_\mu n_\nu m}^* \psi_{n_\mu n_\nu m}|$  in Sec. III to show where the resonance wave functions are located.

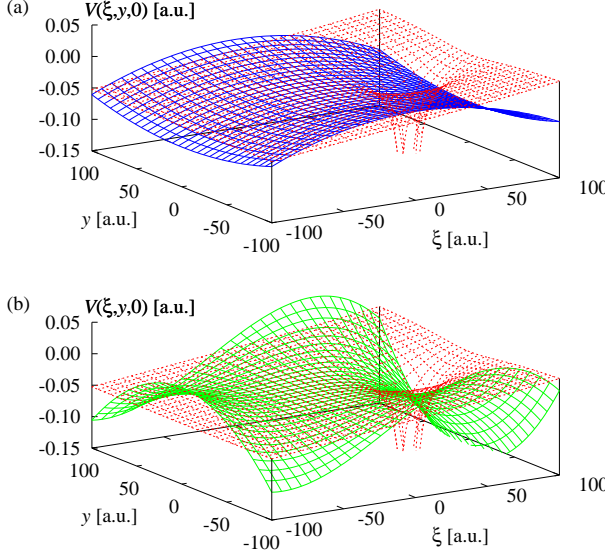


FIG. 1: (Color online) Potential of the hydrogen atom in an external electric field (dashed red grids in (a) and (b)) in comparison with the second-order (a) and third-order (b) power-series expansions around the saddle in the  $(\xi, y)$ -plane with  $\xi = x - x_s$ . Both approximations reproduce the potential the vicinity of the saddle at the origin correctly, however, both are only valid very close to the saddle point.

## B. Approximations in the vicinity of the saddle point

To investigate resonances located at the saddle point, the electric potential of the combined contributions of the nucleus and the external electric field,

$$V_f = -\frac{1}{r} + fx, \quad (11)$$

is expanded into a series up to third-order. As was shown in Ref. [12], already the second-order approximation leads to a good one-to-one correspondence with energies of exact resonances of the full Hamiltonian (1). Here, we additionally consider an approximation including all third-order terms to estimate the quality of the approximation carried out in the vicinity of the saddle point by comparing the second- and third-order results. The saddle point has the coordinates  $\mathbf{r}_s = (-1/\sqrt{f}, 0, 0)^T$  and its energy has the value  $V_f(\mathbf{r}_s) = -2\sqrt{f}$ . Using the coordinate shift  $\xi = x - x_s$  a power-series expansion around  $\mathbf{r}_s$  yields

$$V_f(\mathbf{r}) = -2\sqrt{f} - \sqrt{f}^3 \xi^2 + \frac{1}{2} \sqrt{f}^3 (y^2 + z^2) - f^2 \xi^3 + \frac{3}{2} f^2 \xi (y^2 + z^2) + \mathcal{O}((\mathbf{r} - \mathbf{r}_s)^4). \quad (12)$$

In Fig. 1 the second- and third-order power-series expansions around the saddle point and the full electric potential (11) are compared in the  $(\xi, y)$ -plane. The saddle

structure is clearly visible and the figure demonstrates that both approximations are only valid very close to the saddle point, and thus can describe resonances correctly only in its vicinity.

The approximated Hamiltonian close to  $\mathbf{r}_s$  reads

$$H = \frac{1}{2} (p_\xi^2 + p_y^2 + p_z^2) - \gamma y p_\xi + \frac{1}{2} \gamma^2 y^2 - 2\sqrt{f} + \frac{1}{2} \sqrt{f}^3 (y^2 + z^2 - 2\xi^2) - f^2 \xi^3 + \frac{3}{2} f^2 \xi (y^2 + z^2) + \mathcal{O}((\mathbf{r} - \mathbf{r}_s)^4), \quad (13)$$

where the gauge  $\mathbf{A} = (-\gamma y, 0, 0)$  was used as in Refs. [4, 7, 12], since it leads to a simple structure of the terms. Introducing complex scaling parameters  $s_i$  via

$$\xi = Q_\xi/s_\xi, \quad p_\xi = s_\xi P_\xi, \quad (14a)$$

$$y = Q_y/s_y, \quad p_y = s_y P_y, \quad (14b)$$

$$z = Q_z/s_z, \quad p_z = s_z P_z \quad (14c)$$

we calculate the resonances of the Hamiltonian with the complex rotation method. To do so, a matrix representation with a basis of products

$$|n_\xi, n_y, n_z\rangle = |n_\xi\rangle \otimes |n_y\rangle \otimes |n_z\rangle \quad (15)$$

of one-dimensional harmonic oscillator states  $|n_i\rangle$  is built up and diagonalized.

In the much simpler quadratic approximation, i.e., in the case in which the two third-order terms  $V_3 = -f\xi^3 + 3f^2\xi(y^2 + z^2)/2$  in Eq. (12) are neglected, the approximated Hamiltonian yields a harmonic oscillator spectrum

$$E_{n_z, n_1, n_2} = -2\sqrt{f} + \omega_z \left( n_z + \frac{1}{2} \right) + \omega_1 \left( n_1 + \frac{1}{2} \right) + \omega_2 \left( n_2 + \frac{1}{2} \right), \quad (16)$$

where all frequencies  $\omega_i$  can be calculated analytically [4, 7, 12]. It includes one inverted oscillator, which leads to a purely imaginary frequency  $\omega_2$ , and thus represents the resonance character of the states. The frequency  $\omega_z$  belongs to the  $z$  motion of the electron, whereas  $\omega_1$  and  $\omega_2$  belong to new variables introduced via a canonical transformation [7] to separate the  $x$  and  $y$  motions.

## III. RESULTS AND DISCUSSION

In Ref. [12] it was shown that the energies of some of the resonances calculated in the quadratic approximation around the saddle point agree very well with the exact quantum energies over a large range in the parameter space. The region considered was defined by lines, i.e., one-dimensional objects, in the two-dimensional parameter space to obtain clearly identifiable results. In this

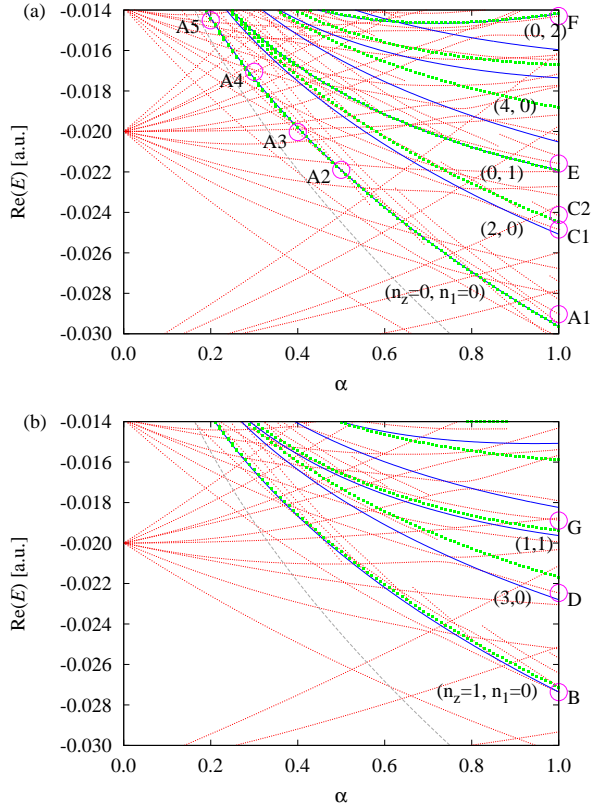


FIG. 2: (Color online) Comparison of the resonance energies (real parts of the complex energy eigenvalues) obtained in exact solutions of the full Hamiltonian (1) (red dotted lines) and the second- (solid blue lines) and third-order (filled green squares) approximations. The results are shown for even (a) and odd (b)  $z$  parity separately. Position space representations of the exact quantum resonances labeled by capital letters are shown in Figs. 3 to 6. In (a) and (b) the dashed grey lines represent the saddle point energy.

paper we chose one of these lines, viz.

$$\gamma = 0.008 \times \alpha, \quad (17a)$$

$$f = 0.0003 \times \alpha, \quad (17b)$$

$$0 < \alpha < 1, \quad (17c)$$

on which all parameters used in what follows are located. Figure 2 shows how the real parts of the resonance energies behave on this line. The red dotted lines represent the exact quantum solution of the full Hamiltonian (1), the solid blue lines and the filled green squares denote the second- and third-order energies, respectively, and the saddle point energy is marked by the dashed grey lines. Results are shown for even [Fig. 2(a)] and odd [Fig. 2(b)]  $z$  parity.

As was already pointed out in Ref. [12] some of the second-order resonances are traced by the exact solutions of (1). Here we see that this is in particular true for all resonances of the second-order power-series expansion (solid blue lines in Fig. 2), which have a clear correspondence in the third-order results (filled green squares in

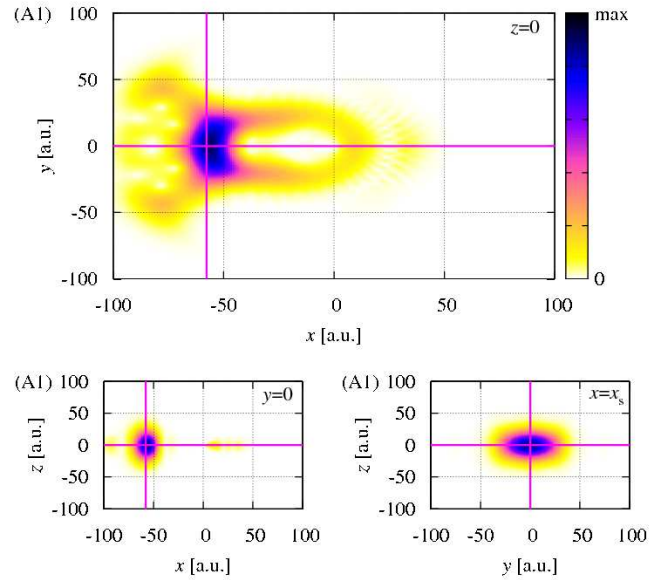


FIG. 3: (Color online) Density plots of the resonance labeled A1 in Fig. 2 in the planes  $z = 0$ ,  $y = 0$ , and  $x = x_s$ . The solid magenta lines mark the saddle point. One can clearly see that the probability density of the resonance is restricted to a close vicinity around the saddle point.

Fig. 2), i.e., which have almost the same energies in both approximations for all parameters  $\alpha$ . In other words, approximated resonances in the vicinity of the Stark saddle point whose energies seem already to be converged in the two lowest-order power-series expansions have also a counterpart in the exact spectrum of the full quantum system described by the Hamiltonian (1). In these cases the simple power-series expansions seem to provide a good approximation for resonances located at the saddle. Due to the very good agreement of the second-order and the exact quantum results in a large region of the parameter space it was already concluded in Ref. [12] that the corresponding exact crossed-fields hydrogen atom resonances must be closely related with localized states predicted by Clark et al.

In this paper we show using the position space representation of the exact quantum wave functions that they are clearly centered at the Stark saddle point in all cases, in which the good agreement in the energies described above appears. The best correspondence is expected for the lowest transition state resonance with quantum numbers  $n_z = 0$ ,  $n_1 = 0$  in the second-order approximation and for the largest field strengths. The position space wave function of this resonance for  $\alpha = 1$ , i.e.,  $\gamma = 0.008$ ,  $f = 0.0003$  (labeled A1 in Fig. 2) is shown in Fig. 3 in the planes  $z = 0$ ,  $y = 0$ , and  $x = x_s$ . All three sections show that the probability density of the resonance is centered at and restricted to a close vicinity of the saddle point, which is marked by the solid magenta lines. The transformation of the quantum resonances corresponding to the same second-order line for decreasing field strengths

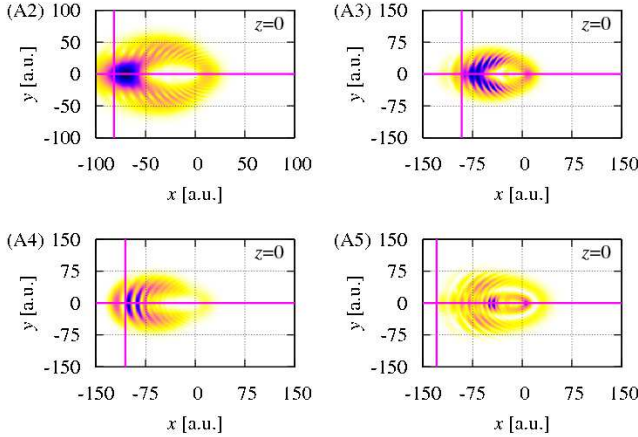


FIG. 4: (Color online) Density plots of the resonances labeled A2, A3, A4, and A5 in Fig. 2 in the  $z = 0$  plane. For decreasing field strengths one can observe that the resonances are decreasingly centered at the saddle point.

can be observed in Fig. 4, where examples for  $\alpha = 0.5$ ,  $\alpha = 0.4$ ,  $\alpha = 0.3$ , and  $\alpha = 0.2$  are drawn in the  $z = 0$  plane. Between  $\alpha = 1$  (resonance labeled A1 in Fig. 2) and  $\alpha = 0.5$  (A2) the shape of the resonance does not change much, it stays centered at the saddle point, however, a radially oscillating probability density at the borders becomes more and more pronounced indicating an increasing contribution of typical Rydberg states. For  $\alpha = 0.4$  (A3) one can already observe that the whole wave function is affected by the oscillations. The influence of the Coulomb potential becomes large enough to lead to a wave function with nodal lines in radial direction for  $\alpha = 0.3$  (A4), whose main maximum is still located at the Stark saddle point. This localization is lost if one decreases the field strengths further, which can be seen for  $\alpha = 0.2$  (A5), where the maximum of the probability amplitude is far away from the saddle.

There are a number of “excited” second-order states which have a correspondence in the third-order power-series expansion as well as in the exact quantum spectrum. Figure 5 compares resonances with excitations in the  $n_z$  quantum number. In the second-order approximation these energies correspond to excited harmonic oscillator states in  $z$  direction. The resonance labeled B represents the quantum number  $n_z = 1$ , i.e., the first excited state. One nodal line at  $z = 0$  is expected in the section and can be observed in Fig. 5. One may argue that a nodal plane at  $z = 0$  is not surprising for a state with odd  $z$  parity, however, further excitations whose nodal patterns reproduce the expectations correctly can be found. Comparing the second-order power-series result for quantum numbers  $n_z = 2$ ,  $n_1 = 0$  and its third-order counterpart in Fig. 2(a) we find two possibilities to assign exact quantum resonances. Indeed, we find the two states labeled C1 and C2 whose probability densities are located very close to the saddle point. Both of these resonances show the two nodal lines expected for  $n_z = 2$  and demon-

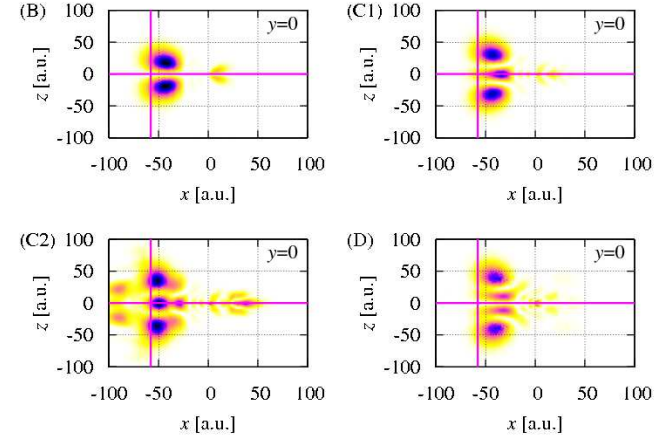


FIG. 5: (Color online) Density plots of the resonances B, C1, C2, and D (cf. Fig. 2) in the  $z = 0$  plane. The resonances can be assigned to second-order approximations with  $n_1 = 0$  and  $n_z \neq 0$ . The nodal patterns expected for excited states in  $z$  direction can be observed.

strate that a rich spectrum of states dominated by the local shape of the potential around the Stark saddle point is present. The resonances C1 and C2 have almost the same real part of the energy but differ significantly in their imaginary parts. One can assume that these resonances can be assigned to two second-order states with  $n_z = 2$ ,  $n_1 = 0$  and different  $n_2$  values, which do not influence the real energy in the second-order approximation. A definite answer, however, is not possible because the excellent agreement in the real parts of the energies of the approximated states with the exact quantum results of the full Hamiltonian (1) does not hold for the imaginary parts [12]. The imaginary parts of the energies obtained with the second- and third-order power-series expansions of the potential do not agree as well as their real parts and cannot be considered converged in these simple approximations. Their quality does not allow for a comparison with their numerically exact counterparts. Note that the exact computations with the complex rotation method provide accurate results for both the real and imaginary parts of the energies. Finally one can even observe the resonance labeled D with three nodal lines as one would expect for a  $n_z = 3$  state, and indeed, the resonance energy can be mapped to that of the second-order state  $n_z = 3$ ,  $n_1 = 0$ . The line belonging to resonance  $n_z = 4$ ,  $n_1 = 0$  in Fig. 2(a) does not seem to have a correspondence in the third-order approximation and it was not possible to find exact quantum resonances with the proper nodal structure.

Further examples including excitations  $n_1 \neq 0$  can be found in Fig. 6. Due to the energy diagram in Fig. 2(a) resonance E can be assigned to quantum numbers  $n_z = 0$ ,  $n_1 = 1$ . The position space representation in Fig. 6 reveals a complicated shape of the probability density, which is not very surprising as the excitation in  $n_1$  belongs to a coordinate whose origin is in a canonical

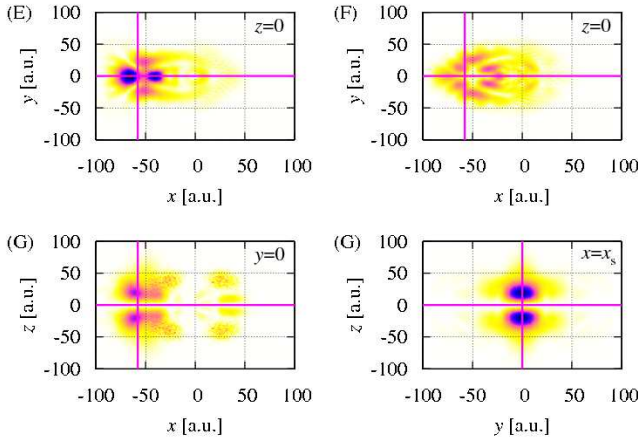


FIG. 6: (Color online) Density plots of the resonances E, F, and G (cf. Fig. 2) corresponding to states of the quadratic approximation excited in  $n_1$ . Complicated nodal patterns are found.

transformation including the positions  $x, y$  as well as the momenta  $p_x$  and  $p_y$ . However, the resonance is clearly located close to the position of the saddle. This is also true for resonance F, which is assigned to the second-order quantum numbers  $n_z = 0, n_1 = 2$  and shows even a more complicated nodal pattern in position space. Resonance G is connected with an excitation in both  $n_z$  and  $n_1$  ( $n_z = 1, n_1 = 1$ ) and exhibits a nodal plane at  $z = 0$  due to the respective quantum number  $n_z = 1$ .

#### IV. CONCLUSION

By determining the position space representation of quantum mechanically exact wave functions we have proved the existence of resonances located in a close vicinity of the Stark saddle point which were predicted by simple classical approximations as, e.g., the transition state theory. The results show that near the saddle one can find a spectrum of several states belonging to the local neighborhood of the saddle and ignoring the global structure of the Coulomb potential. It reproduces the

expectations of a simple quadratic power-series expansion around the saddle in the energies as well as in the shape of the wave functions. In particular, one can, in the quadratic approximation, separate three one dimensional harmonic oscillators one of which is connected with the  $z$  direction. In this spatial direction we found nodal planes of resonances which have the structure of ground and excited states from  $n_z = 0$  up to  $n_z = 3$ . Complicated nodal patterns are found for excitations in the quantum number  $n_1$  not directly connected to a spatial coordinate.

The comparison of the two approximations of the resonance energy eigenvalues (cf. Fig. 2) showed that some of the second-order energies have a distinct correspondence in the third-order approximation while some have not. In all cases in which an assignment of the results of both approximations is possible we were also able to detect an exact quantum resonance with a strong localization at the saddle, whereas such a strong connection to the saddle could not be observed for exact resonances not belonging to a pair of second- and third-order resonances. Despite this clear result it must be noted that, as was already pointed out in a previous publication [12], the simple power-series expansions are not capable of reproducing the resonance widths (or imaginary parts of the energy eigenvalues) correctly. We have demonstrated, however, that a convergence of the approximated resonance energies (or real parts) is already a strong signature of the existence of exact quantum states centered at the saddle.

The results prove that resonances located at an outer saddle predicted in a variety of theoretical work [1, 2, 4, 5, 7] and supported by experimental results [6] do exist in the Coulomb potential superimposed by two external fields. The correspondence already appears for very simple second- and third-order power-series expansions of the potential at the saddle point. For future work comparisons with more thorough approximations applicable to the problem, e.g., the normal form expansion developed for identifying the classical transition state in high-dimensional systems [7, 10, 11] or its quantum analogue [11, 18] will be of high value.

---

[1] S. K. Bhattacharya and A. R. P. Rau, Phys. Rev. A **26**, 2315 (1982).  
[2] J. C. Gay, L. R. Pendrill, and B. Cagnac, Phys. Lett. A **72**, 315 (1979).  
[3] A. R. P. Rau and L. Zhang, Phys. Rev. A **42**, 6342 (1990).  
[4] C. W. Clark, E. Korevaar, and M. G. Littman, Phys. Rev. Lett. **54**, 320 (1985).  
[5] M. Fauth, H. Walther, and E. Werner, Z. Phys. D **7**, 293 (1987).  
[6] G. Raithel, M. Fauth, and H. Walther, Phys. Rev. A **47**, 419 (1993).  
[7] T. Uzer, C. Jaffé, J. Palacián, P. Yanguas, and S. Wiggins, Nonlinearity **15**, 957 (2002).  
[8] C. Jaffé, D. Farrelly, and T. Uzer, Phys. Rev. Lett. **84**, 610 (2000).  
[9] C. Jaffé, D. Farrelly, and T. Uzer, Phys. Rev. A **60**, 3833 (1999).  
[10] S. Wiggins, L. Wiesenfeld, C. Jaffé, and T. Uzer, Phys. Rev. Lett. **86**, 5478 (2001).  
[11] H. Waalkens, R. Schubert, and S. Wiggins, Nonlinearity **21**, R1 (2008).  
[12] H. Cartarius, J. Main, and G. Wunner, Phys. Rev. A **79**, 033412 (2009).  
[13] J. Main and G. Wunner, J. Phys. B **27**, 2835 (1994).

- [14] W. P. Reinhardt, *Ann. Rev. Phys. Chem.* **33**, 223 (1982).
- [15] D. Delande, A. Bommier, and J. C. Gay, *Phys. Rev. Lett.* **66**, 141 (1991).
- [16] N. Moiseyev, *Phys. Rep.* **302**, 212 (1998).
- [17] T. N. Rescigno and V. McKoy, *Phys. Rev. A* **12**, 522 (1975).
- [18] R. Schubert, H. Waalkens, and S. Wiggins, *Phys. Rev. Lett.* **96**, 218302 (2006).